

APPLICATION NOTE

Amplitude and Phase Characterization of Ultrashort Laser Pulses

33

Technology and Applications Center
Newport Corporation

“In order to measure an event in time, you need an even shorter event.”

Rick Trebino, Inventor of Frequency Resolved Optical Grating.

1. Introduction

As a consequence of the time-bandwidth uncertainty principle, ultrashort laser pulses carry significant bandwidth. If the spectral components that fall under the bandwidth of the laser pulse are time coincident (figure 1.1), the pulse is said to be at its transform limit. A transform-limited pulse implies that the pulse duration is minimized.

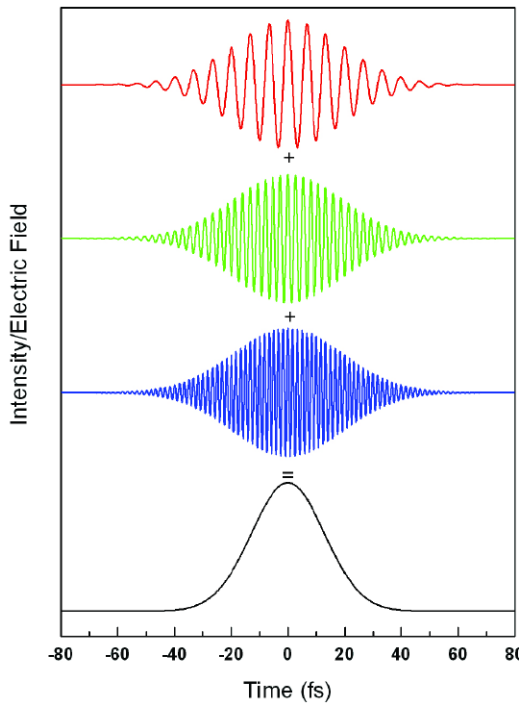


Figure 1.1: The temporal relationship between selected Fourier components of a transform-limited pulse.

Material properties, such as dispersion, alter the (phase) relationship between the spectral components of light, effectively separating the blue and red components of the pulse in time (figure 1.2). This effect is known as chirp, and for an ultrashort pulse, serves to elongate the pulse in time. Although autocorrelation (see Application Note 27 – Long Scan Autocorrelator www.newport.com/AppsNote27) can measure the duration of an ultrashort pulse, it is unable to characterize the phase relationship between different spectral components. The primary reason for this is that autocorrelators utilize a single element photodetector that effectively integrates over the spectral profile of the pulse.

Fortunately, techniques exist that monitor the spectral profile of a pulse as a function of time. These techniques allow for

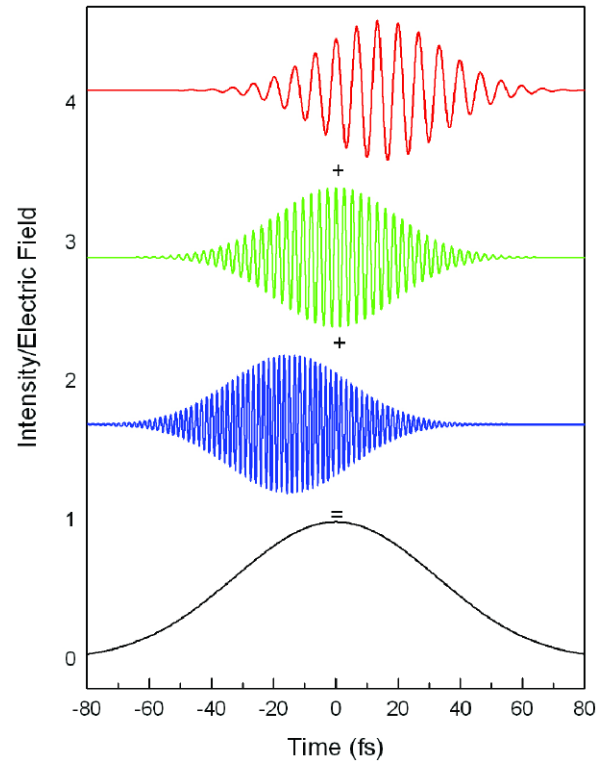


Figure 1.2: The temporal relationship between selected Fourier components of a positively chirped pulse.

the complete reconstruction of the electric field. Of these techniques, frequency-resolved optical gating (FROG) is arguably the most straightforward and easiest to implement. As mentioned earlier, FROG allows for full phase retrieval of the input field without the ambiguity associated with autocorrelation. This note presents a simple, low dispersion, easy-to-use, general purpose FROG device that can be readily implemented on the Newport Long Scan Autocorrelator platform as described in Application Note 27.

FROG is a general technique and can be employed in a variety of experimental geometries, a few of which are listed in Table 1.¹

Table 1: Various FROG geometries with associated pros and cons.

FROG Geometry	Works with Oscillator	Works with Amplifier	Characterize Sign of Chirp	Relative Complexity
SHG FROG (Second Harmonic)	Yes	Yes	No	Low
THG FROG (Third Harmonic)	Yes	Yes	Yes, but not intuitive	High
TG FROG (Transient Grating)	High Powered Only	Yes	Yes	High
PG FROG (Polarization Gate)	No	Yes	Yes	High
SD FROG (Self Diffraction)	No	Yes	Yes	Moderate

Each geometry has certain advantages as well as limitations which need to be considered within the context of the laser pulse to be measured. In this note, we focus on two geometries: self-diffraction FROG (SD FROG) for amplified systems and second harmonic FROG (SHG FROG) for oscillators. The SD FROG trace gives an intuitive picture of the pulse (i.e. the direction of time is preserved), which is a highly desirable feature for real-time laser alignment. Moreover, the geometry is identical to the Long Scan Autocorrelator where the nonlinear medium is a thin piece of glass ($<200\mu\text{m}$), thus making this geometry cost effective and straightforward to implement. On the downside, SD FROG requires relatively high peak powers not readily available from most ultrafast oscillators, so its use is restricted to amplified systems. For oscillators, the only real option is SHG FROG.¹ An SHG FROG is simply a spectrally resolved autocorrelator. Although the sign of the spectral phase is lost in the measurement, efficient algorithms exist which can deduce the order and magnitude of the spectral phase where the sign can be determined if needed by performing additional measurements.¹

2. SHG FROG

Figure 2.1 illustrates a block diagram of the SHG FROG device. An incoming pulse, $E(t)$, is first split into two replicas by means of an ultrafast beamsplitter.

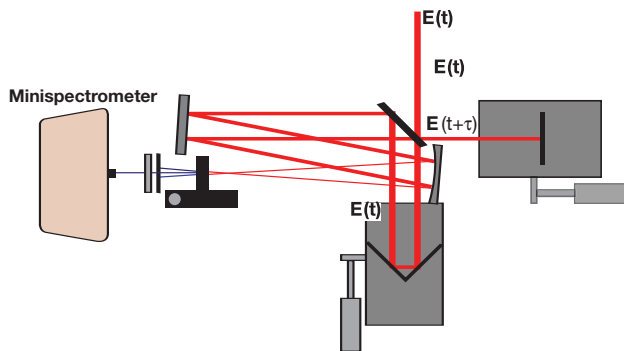


Figure 2.1: Diagram of SHG FROG setup.

The two replicas are sent down two independent delay lines, one variable and one fixed, in order to generate a time delay, τ , as well as to introduce a spatial offset between the two beams. In order to avoid the dispersive effects of a lens, the two replicas, $E(t)$ and $E(t+\tau)$, are directed to a spherical mirror and then focused into a nonlinear crystal (BBO) capable of generating a second harmonic signal. The two-beam second harmonic signal, phase matched such that it appears directly between the two beams, is isolated by means of an iris and sent to a spectrometer. The spectrum is recorded as a function of delay, $I_{\text{SHG}}(\omega, \tau)$, and can be described by the following equation:

$$I_{\text{SHG}}(\omega, \tau) \sim \int I(t)I(t+\tau)e^{-i\omega\tau} dt \quad (1)$$

It is worth noting that since only intensities are involved in equation (1), the sign of the spectral phase is lost in this measurement.

To illustrate the output of an SHG FROG, let us consider a 20 femtosecond pulse centered at 600 nm corresponding to the typical output of a noncollinear optical parametric amplifier (NOPA). Figure 2.2 illustrates the SHG FROG trace for a pulse before and after it travels through a dispersive medium having $+468 \text{ fs}^2$ of group delay dispersion (GDD) and $+282 \text{ fs}^3$ of third order dispersion (TOD) (i.e. 2 mm of SF10 glass at 600 nm). Initially, the pulse is transform limited at 20 fs (2.2a). Figure 2.2b shows the pulse after traveling through the material. The pulse, symmetric about the time origin, is now elongated in time to 129 fs. The integrated bandwidth profile remains unchanged. The symmetry of the chirped pulse is due to the fact that only intensities are involved in this process (i.e. the square of the electric field). Figures 2.2c and 2.2d illustrate the individual contributions of GDD and TOD to the overall chirped profile. The GDD term is primarily responsible for elongating the pulse in time. The TOD term skews the distribution of frequencies in time, creating the non-elliptical FROG trace. By itself, the SHG FROG trace containing only TOD still retains the “horseshoe” pattern characteristic of third order dispersion. This highlights the fact that this technique can delineate GDD from higher order dispersion even though their signs are not extractable.

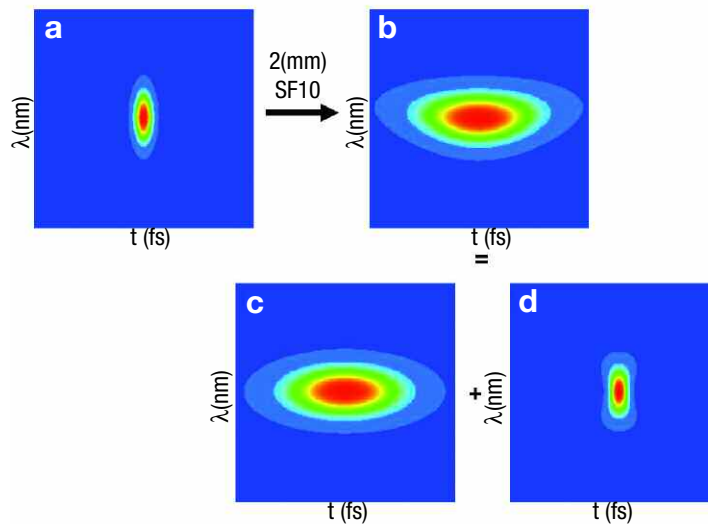


Figure 2.2: SHG FROG traces for a 20 fs pulse before (a) and after (b) traveling through a dispersive medium. Insets (c) and (d) show the individual contributions of group delay dispersion and third order dispersion respective.

In contrast with the Long Scan Autocorrelator, the only dispersive element used is either the 3mm ultrafast beamsplitter or the $5 \mu\text{m}$ pellicle beamsplitter. This is done to minimize the dispersion of the device. The SHG FROG can be readily converted into a low dispersive autocorrelator by simply inserting a photodetector just prior to the spectrometer.

3. SD FROG

Figure 3.1 illustrates a block diagram of the SD FROG device. The set up is quite similar to the SHG FROG setup. As with the SHG FROG, an incoming pulse, $E(t)$, is first split into two replicas by means of a pellicle beamsplitter.

Warning, A 5 μm pellicle beamsplitter is recommended to limit the unbalanced dispersion introduced by this optic due to the asymmetry of the two arms. The pellicle is not recommended for the oscillators, due to the high average power needed to achieve reasonable pulse energies required to drive the nonlinear process. These average powers can exceed the damage threshold of the pellicle.

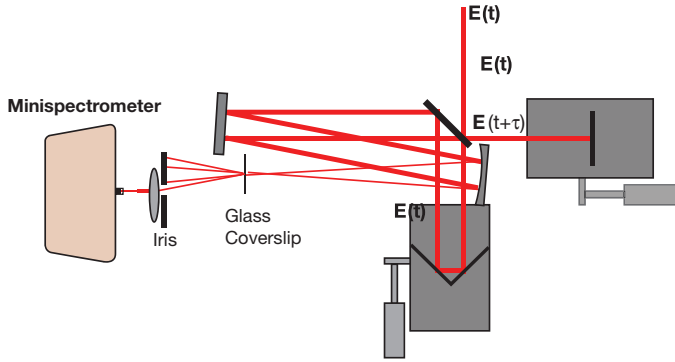


Figure 3.1: Diagram of SD FROG setup.

The two replicas are sent down two independent delay lines, one variable and one fixed, in order to generate a time delay, τ , as well as to introduce a spatial offset between the two beams. The two replicas, $E(t)$ and $E(t+\tau)$, are directed to a concave spherical mirror and then focused into a thin nonlinear medium. For this application, the nonlinear medium is a borosilicate glass coverslip (~ 200 microns thick) which generates the self-diffraction signal. The self-diffraction signal, which appears to either side of both beams, is isolated by an iris and then focused into the spectrometer by a lens. The spectrum is recorded as a function of delay, $I_{SD}(\omega, \tau)$, and can be described by the following equation:

$$I_{SD}(\omega, \tau) \sim \left| \int [E(t)^2 + E(t - \tau)] e^{-i\omega t} dt \right|^2 \quad (2)$$

Unlike the analogous equation describing SHG FROG, equation 2 has a term corresponding to the direct electric field with phase intact. This property allows for the full retrieval of spectral phase. Moreover, the SD FROG traces are highly intuitive. The 20 fs pulse mentioned above illustrates how the SD FROG measures the pulse. Figure 3.2a shows a simulated SD FROG trace for a transform-limited 20 fs pulse

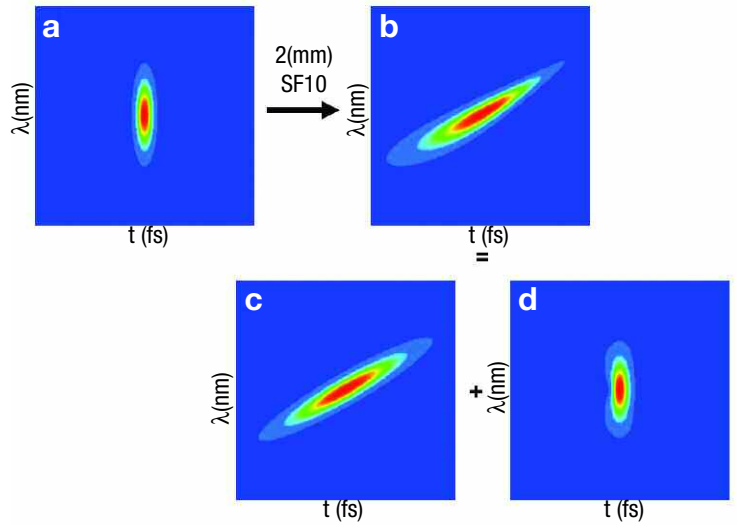


Figure 3.2: SD FROG traces for a 20 fs pulse before (a) and after (b) traveling through a dispersive medium. Insets (c) and (d) show the individual contributions of group delay dispersion (GDD) and third order dispersion (TOD) respectively.

using equation 2. It appears similar to the SHG FROG trace shown in figure 2.2a. However, when material dispersion is added to the pulse ($+468 \text{ fs}^2$ and $+282 \text{ fs}^3$ shown in figure 3.2b), the SD FROG trace becomes asymmetric. Figures 3.2c and 3.2d show the individual contributions of GDD and TOD to the SD FROG trace. Again, GDD is primarily responsible for elongating the pulse in time (the physics remains unchanged). However, this SD FROG trace is not symmetric about the time origin. Figure 3.2c clearly shows that the red frequencies are advanced in time with respect to the blue frequencies, as is the case with positive GDD. Figure 3.2d shows the contribution of third order dispersion. Similar to the SHG FROG, the SD FROG trace also displays a “horseshoe” pattern which is the signature of cubic chirp. However, the skewing of the pulse only occurs at the leading edge of the pulse, which is characteristic of positive TOD. It should be clear from these figures that the electric field in its entirety is extractable from this technique, which makes it the geometry of choice when sufficient pulse energies are available.

Self-diffraction differs from second harmonic generation. In equation 2, the electric field appears three times on the right hand side of the equation. This implies that the generation of the observable signal involves three time ordered interactions of the electric field. Intuitively, one may think of first two interactions of the electric field as forming a transient grating (the origin of which will be discussed in the next paragraph). The observable signal is then the portion of the third field diffracted by the transient grating.

The origin of the transient grating arises from the high peak intensity of the laser pulse coupled with the overlap of the two beams. In the case where two coherent beams overlap at an angle, the wavefronts undergo constructive and destructive interference producing a periodic variation in intensity as shown in figure 3.3. For an isotropic medium in the weak field limit, the refractive index is uniform across the medium and unaffected by the interference pattern. However, in the presence of a strong field, as is the case with an ultrashort pulse, the effective refractive index, n_{eff} , is modified in the regions of constructive interference according to the expansion shown below¹,

$$n_{eff} = n_0 + n_2 I \dots \quad (3)$$

where the higher order terms are due to the interactions between the intense laser pulse and the electrons of the medium (induced nonlinear polarization). So, when the two fields overlap (at an angle) in time and space, they produce a periodic variation in refractive index. This is exactly a diffraction grating, which is a function of intensity and therefore a function of time (hence the term “transient grating”). While this transient grating is established, incident beams partially diffract from it, producing the self-diffraction signal. This process can be thought of as an electric field diffracted from an intensity grating.

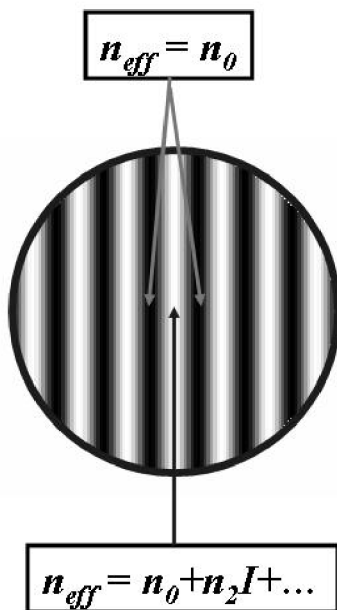


Figure 3.3: Intersection of two ultrashort pulses at an angle. The dark areas correspond to regions of destructive interference and the light areas correspond to regions of constructive interference. The intensity of the pulse modifies the refractive index in the regions of constructive interference such that a transient grating is established when the pulses overlap in time.

It is also worth noting that in this geometry, the self-diffraction process is not properly phase matched.¹ Phase matching occurs when all the wave vectors, k -vectors, involved in the nonlinear process sum up to zero. The k -vector is a term in the electric field that describes the propagation direction of the field with magnitude given by,

$$k = \frac{n\omega}{c} \quad (4),$$

where n is the refractive index of the material, ω is the frequency of the light and c is the speed of light.

As mentioned earlier, self-diffraction (SD) is generated through the interaction of three fields. Likewise, the direction of the SD field, given by the k -vector, will be determined by the interaction of the three fields,

$$k_{SD} = 2k_P - k_{P'} - \Delta k \quad (5),$$

where k_{SD} is the k -vector representing the SD field, k_P and $k_{P'}$ are the k -vectors representing the two spatially distinct input fields and Δk is the phase mismatch. Figure 3.4 illustrates the k -vector diagram for the self-diffraction process. The direction of the input fields based on simple vector addition of the input fields based on equation 5. Since the medium is isotropic and the frequencies are all the same, the lengths of all the k -vectors are identical. As illustrated in figure 3.4, there is a gap between k_{SD} and $2k_P - k_{P'}$. This is the phase mismatch inherent to this process and is an increasing function of the angle between the two beams as well as the interaction length in the nonlinear medium. It is for this reason that the angle between the two beams should be at a minimum. Moreover, the nonlinear medium must be thin to avoid complete destructive interference between the SD fields generated from different points within the interaction volume.

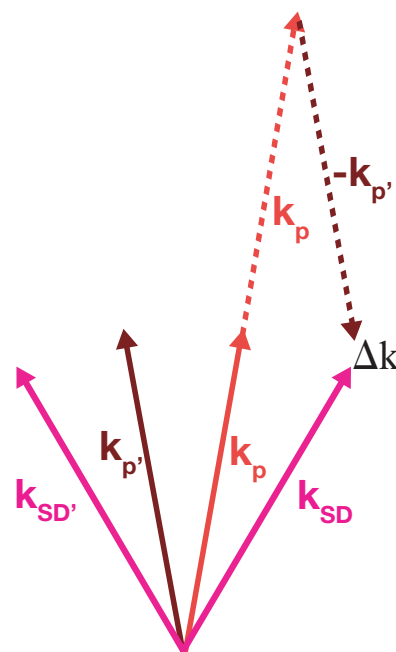


Figure 3.4: Wave vector diagram for self-diffraction. The wave vector for the self-diffraction signal is given by $k_{SD} = 2k_P - k_{P'}$.

Also shown in figure 3.4 there are the two SD fields generated in the nonlinear medium, denoted by k_{SD} and k_{SD}' . k_{SD} and k_{SD}' are generated from the electric fields formed by the P and P' pulses, respectively, diffracting from an intensity grating formed between the two pulses. Care must be taken when choosing which SD field to monitor. In order to preserve the direction of time, the monitored SD field should correspond to the one generated by the input field of the pulse on the motorized delay line (i.e. if the motorized delay line is on the P' field, then the SD' field should be the field monitored). If this is not done, the direction of time will be reversed, and the time sequence of the individual spectra that make up the FROG trace will need to be inverted.

4. Data Analysis

Unlike the analogous equation for autocorrelation, no closed form solution exists for equations 1 or 2. This significantly complicates data analysis which at a minimum must involve an iterative method incorporating a 2D phase retrieval algorithm.¹ Fortunately, efficient algorithms for phase retrieval exist and are available from Femtosec Technologies. The output from the software provided with this kit can be directly imported into Femtosec's FROG 3.0 software without modification.

5. Building the Subassemblies

WARNING!! - Visible and invisible radiation emitted by laser devices can be dangerous to the eyes and appropriate precautions must be taken when lasers are in use. Only individuals who are adequately trained in proper laser use and safety procedures should operate the laser devices described herein.

Detailed diagrams for building the subassemblies of the SHG and SD FROG are presented in the Appendix. When building Delay Line 1 (Assembly 1), the silver mirrors should be glued to the mirror mounts using epoxy glue (not included). Make sure that the two mirrors are positioned at a 90° angle with respect to each other and at a 45° angle with respect to the plane of the optical table. This is the correct orientation for the mirrors if the laser beam is horizontally polarized (If the laser is polarized in the vertical direction, $\lambda/2$ wave-plate should be used to rotate the polarization). This assembly is meant to provide a vertical displacement to the incoming beam. When aligned correctly, the direction of the outgoing beam will be independent of stage position.

6. Routing the Beam

The beam must be routed from the laser to the intended location of the FROG, before the device is actually built. Two routing mirrors are necessary to ensure that the beam is at the correct height and level to the optical table (see Application Note 27 – Long Scan Autocorrelator).

7. Assembling the FROG SHG FROG

At this point, it is useful to construct an alignment tool using the parts from the Iris Assembly. The Iris Assembly should be aligned such that the beam is centered in the middle of the iris immediately after the second routing mirror (see figure 7.1).

Using the hole pattern on the optical table as a guide, the iris should be moved in a straight line far from the 2nd routing mirror (see figure 7.2). Using the tip/tilt adjustment on the 2nd routing mirror, center the beam on the iris. Repeat this procedure iteratively until the beam travels parallel to the hole pattern of the table.

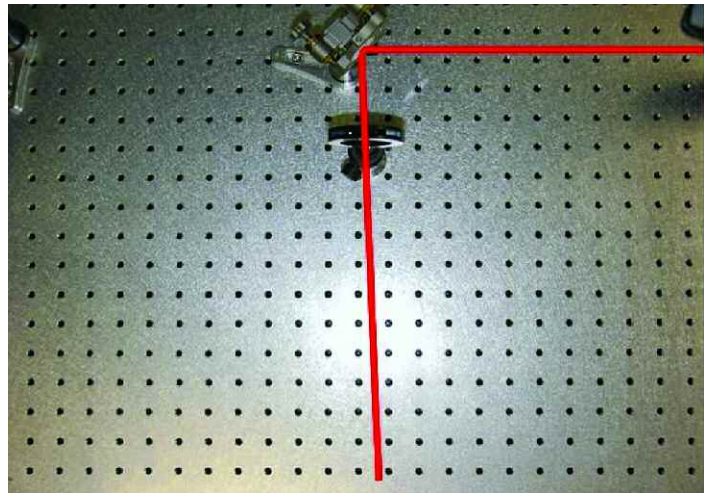


Figure 7.1: Pre-alignment of the beam into the FROG.

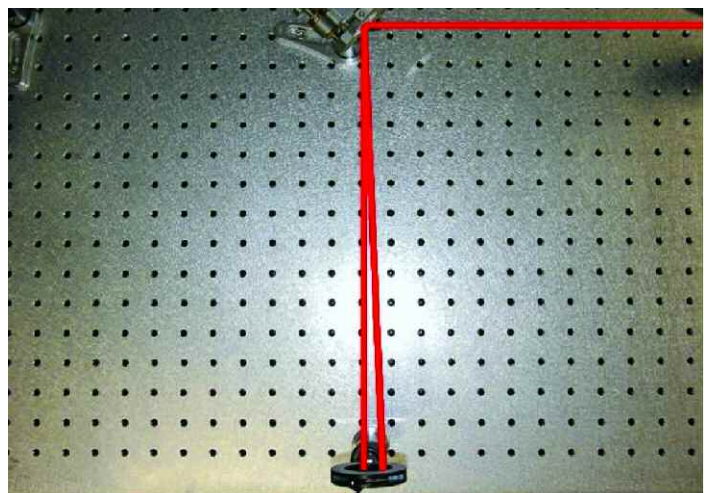


Figure 7.2: Alignment of the beam with respect to the table.

Position the Delay Line 1 Assembly at least 200 mm behind routing mirror 2 such that the beam is centered on both mirrors (see figure 7.3).

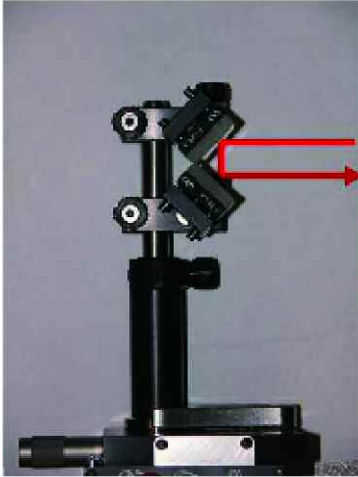


Figure 7.3: Alignment of two mirrors on Delay Line 1.

Using the two routing mirrors, ensure that the beam is traveling at a constant height and parallel to the axis of motion of the stage. The beam should hit the center of the top mirror and reflect from the center of the bottom mirror. The beam exiting the delay line should travel parallel to the incoming beam with a vertical displacement of approximately 25 mm (see figure 7.4). The exiting beam should not translate with position of the stage.

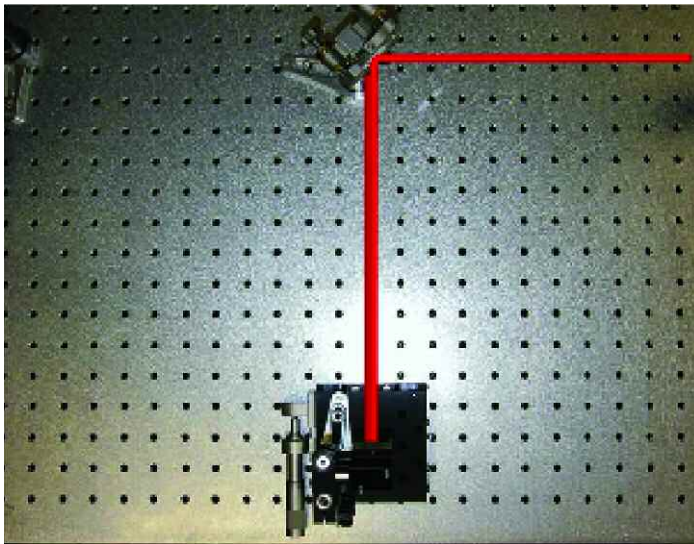


Figure 7.4: Alignment of Delay Line 1.

WARNING, average powers greater than $1\text{W}/\text{cm}^2$ will result in catastrophic damage to the pellicle beamsplitter. Care should be taken to attenuate the beam if necessary.

Insert the Beamsplitter Assembly between routing mirror 2 and Delay Line 1 (see figure 7.5). The center of the beamsplitter should be approximately 100 mm from the edge of the stage. The beam should be centered vertically on the beamsplitter approximately 1 cm from the top. Using the tip/tilt adjustments on the Beamsplitter Assembly, ensure that the reflected beam travels at a constant height and is completely perpendicular to the axis of motion of Delay Line 1 (see figure 7.6). Use the procedure described above utilizing the Iris Assembly as a target.

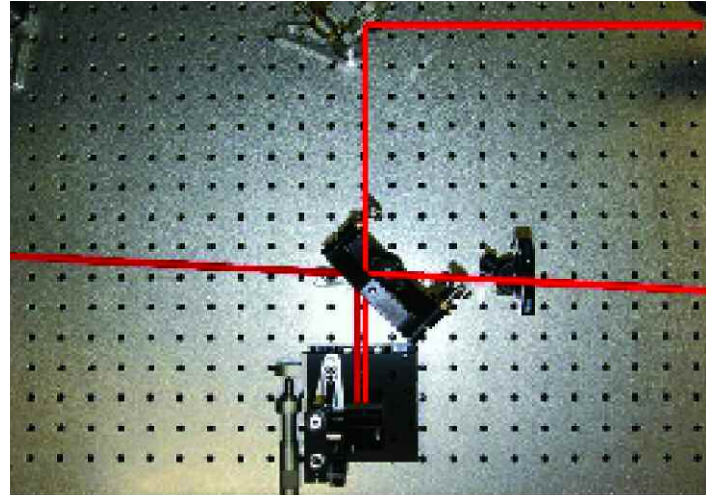


Figure 7.5: Positioning of the beamsplitter (pellicle shown).

Insert Delay Line 2 approximately 115 mm behind the Beamsplitter Assembly. Using the tip/tilt adjustments on the mirror mount, ensure that this beam travels back on itself. After the beamsplitter, verify that the two beams corresponding to the two arms of the autocorrelator are displaced vertically by approximately 25 mm and are traveling parallel to each other as well as the table.

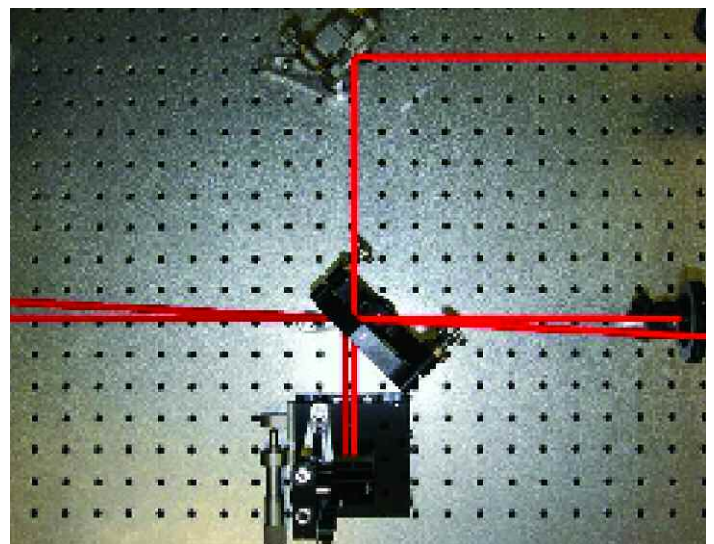


Figure 7.6: Alignment of the beamsplitter (pellicle shown).

Insert the Folding Mirror Assembly approximately 250 mm after the beamsplitter. Adjust the mirror height and position such that both beams hit the surface of the mirror without clipping. Place the Spherical Mirror Assembly on the adjacent side of the beamsplitter (see figures 7.7a and 7.7b). Using the Folding Mirror Assembly, route the two beams to the Spherical Mirror Assembly such that the two beams are centered on the vertical axis of the mirror and balanced on the horizontal axis. The two beams should overlap in tight focus approximately 250 mm behind the spherical mirror. If the two beams do not overlap in tight focus, use the tip/tilt adjustment on the Delay Line 2 mirror to overlap them.

Insert the Crystal Assembly approximately 250 mm after the lens at the intersection of the two beams. Make sure that the principle plane of the crystal is oriented at 90 degrees with respect to the polarization plane of the incoming beam (horizontally polarized light should be used with this configuration, otherwise the rotation stage should be flipped 90°). Place the dichroic filter immediately after the crystal. Using a sheet of white paper for viewing purposes, rotate the crystal until the second harmonic of one of the two beams becomes visible on the paper (note the angle). Continue rotating the crystal until the second harmonic of the second beam becomes visible (note the angle). The phase-matching angle for two-beam second harmonic is the half point between these two angles. Set the crystal angle to this half point.

Scan the two delay lines until a time dependent second harmonic signal can be observed between the two beams. This is a delicate procedure, which may involve several iterations of overlapping the two beams spatially in the crystal followed by scanning the two delay lines. Once the two-beam second harmonic is found, aperture it with the Iris Assembly such that no additional contribution from the single beam second harmonic is passing through the iris. Place the Spectrometer Assembly as close to the iris as possible. Center the second harmonic on the entrance slit of the spectrometer by translating the spectrometer assembly. Insert the second Iris Assembly into the beam path prior to the beamsplitter. Center the iris with respect to the beam. Aperture the beam using the iris such that the second harmonic signal is not saturated. When completed, the SHG FROG should resemble that shown in figure 7.7a.

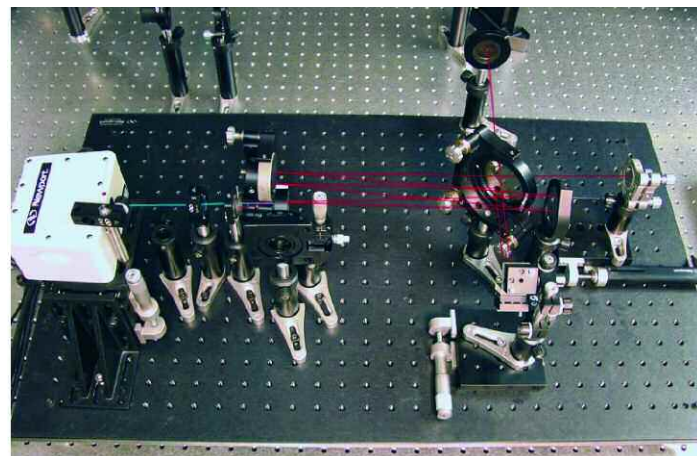


Figure 7.7a: Apparatus for measuring the SHG FROG

As mentioned earlier, the SHG FROG can be converted into a minimally dispersive autocorrelator by inserting a photodetector before the spectrometer. This option is shown in Figure 7.7b using Newport's 918UV detector attached to the 1918-C hand held power meter, which is used for data acquisition.

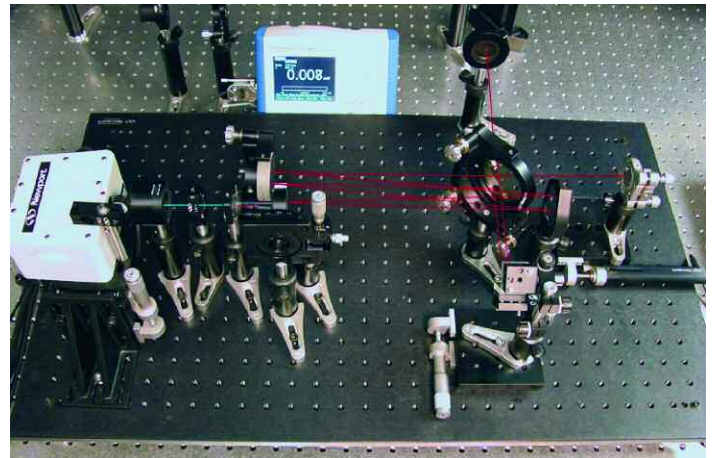


Figure 7.7b Converting the SHG FROG to a minimally dispersive autocorrelator.

SD FROG

WARNING, overlapping the beam in time and space using the self-diffraction signal is extremely difficult. Therefore, it is recommended that the user first build the SHG FROG as a starting point.

Block the beam and remove the Crystal Assembly as well as dichroic filter. Insert the Thin Glass Assembly into the beam path such that the glass is at the same location as the BBO crystal. Block the spectrometer entrance and unblock the beam. At this point, it may prove useful to dim the lights. Translate the glass in and out of focus until the spot size in the glass is minimized. Secure the Thin Glass Assembly. Open or close the iris prior to the beam splitter such that the pulse energy is just below the white light threshold in the glass. Using the tip/tilt adjustment on the mirror mount in Delay Line 2, overlap the beams in the glass (an IR viewer will be necessary if working in the NIR and IR spectral regions). Place a white card after the Glass Assembly. Translate both arms of the interferometer while monitoring the card for the appearance of the self-diffracted signals both above and below the input beams. The self-diffraction signal will be at the same frequency as the laser. If no signal is observable, repeat this step. (Note, it is normal to repeat this step several times before observing the self-diffraction signal.)

Once the self-diffraction is observed, aperture it with the Iris Assembly such that no contributions from the input beams are passing through the iris. Insert the second lens assembly (Lens Assembly 2) immediately after the iris and translate the Spectrometer Assembly such that the self-diffraction is focused at the entrance port of the spectrometer. When completed, the SHG FROG should resemble that shown in figure 7.8.

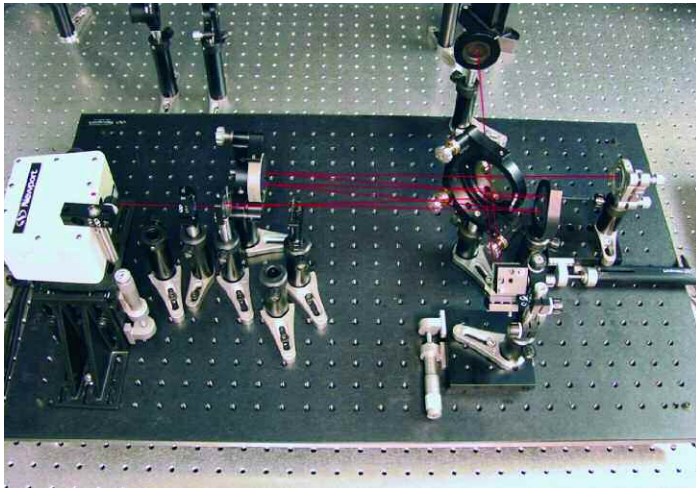


Figure 7.8: Apparatus for measuring the SD FROG.

8. Running the Software

WARNING, the operating system tested with this device is Windows XP Professional Edition. Newport does not guarantee compatibility with other operating systems.

Prior to connecting any device, install the software according to the procedure specified on the installation disk. Connect the spectrometer to the computer through the USB port located on the side of the spectrometer. Connect the SMC100CC controller to the computer using the RS232 cable provided. Run the SMC100CC program from the Start Menu. Make sure the stage is properly configured and sent to the home position. Command the stage to its center position (12.5 mm). Note the COM port address. Close the SMC100CC program. After successful completion of this step, a green LED should be illuminated on the SMC100CC controller. If it is not, the SMC100CC controller is not properly configured and the device will not function. If this is the case, consult the User Manual. Next, run the MiniSpec Tracq program from the Start Menu and acquire data. Make sure that the spectrometer is capable of “seeing” light. If the SHG or SD signal saturates the spectrometer, decrease the integration time until the spectrometer is no longer saturated. The minimum integration time is 1 ms. If the spectrometer saturates at this setting, further attenuation of the beam is necessary and can be easily accomplished by

reducing the aperture of the iris prior to the beamsplitter.

Run the Newport UPC program from the Start Menu. Upon opening the program, the user will be prompted to enter the COM port address for the SMC100CC motion controller (see figure 8.1). Enter the value noted above and click on the Continue button.

Click on the Start Spectrum button. The program will immediately start collecting spectra as shown in figure 8.2 (the translation stage is idle at this point). Set the home position to the same center stage position (12.5mm) as used in the previous step for the SMC100CC software. Click on the Goto Home button. Set the integration time, start wavelength, stop wavelength, total delay and target resolution (time resolution). The dead time should be initially set to 20 ms.



Figure 8.1: Setting the COM port address.

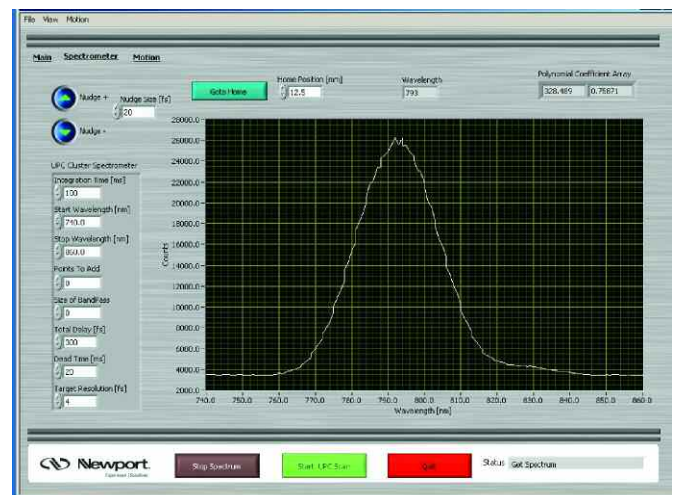


Figure 8.2: Spectrometer mode.

Using the up and down arrows, the user can jog the stage by a user defined increment (Nudge Size). This feature is useful for estimating the pulse duration. Using the reverse arrow (pointing down), position the stage such that the spectrum falls to the level of the noise (see figure 8.3). It is important that the noise spectrum is free from the real signal since the former will automatically be subtracted from each subsequent spectrum collected during the FROG measurement.

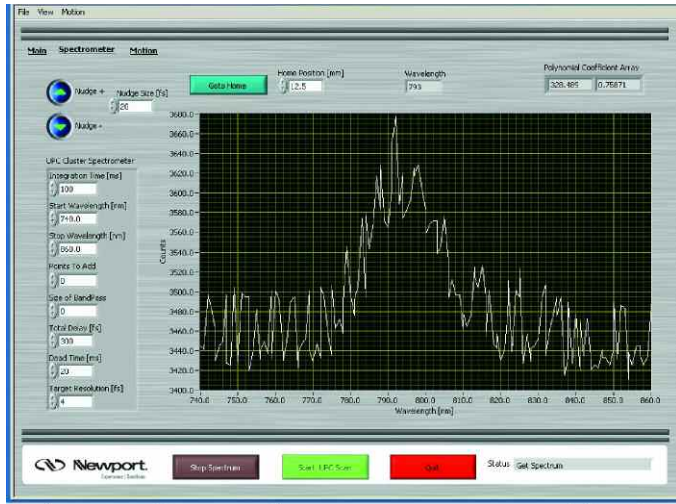


Figure 8.3 Jog the stage using the (Nudge -) button until the time dependent signal vanishes. This “background” spectrum will be subtracted from the FROG measurement. Stray light may introduce some background component as illustrated in the figure.

Click on the Stop Spectrum button to stop collecting spectra. In the upper left hand corner, click on Main to switch to the data collection screen (figure 8.4).

Press the Start UPC Scan button. The program will start acquiring FROG data. In order to prevent the effects of backlash, the program collects data only while the stage is moving forward (i.e. the actuator is pushing the stage). The FROG parameters displayed on this screen can be modified anytime. However, if they are modified during the scan, that scan may appear distorted. The data can be saved at anytime by pressing Ctrl+S. The data will be automatically named based on a time stamp and saved to user specified folder. The format of the data is compatible with Femtsoft’s FROG 3.0 software. The data is stored as a series of spectra where the first five points in the file represent: (1) the number of delay points, (2) the number of wavelength points, (3) femtoseconds per pixel, (4) nanometers per pixel and (5) wavelength of center pixel. Figure 8.4 (close to transform limit) and figure 8.5 (positively chirped pulse) show some sample SD FROG traces taken at the Technology and Applications Center in Irvine, CA.

Finally, clicking on the Motion button takes the user to an SMC100CC diagnostic utility which allows the user to manually issue commands to the SMC100CC controller as well as to read back from it. It should be used only after consulting the SMC100CC User Manual.

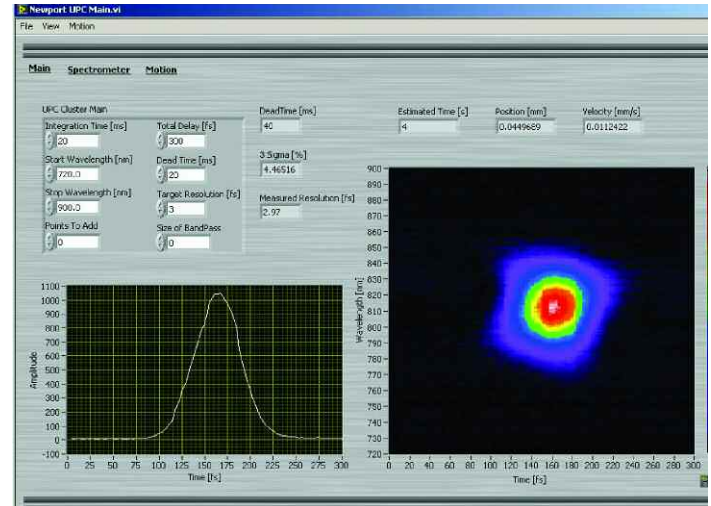


Figure 8.4 Main window. The SD FROG trace corresponds to a pulse at its temporal profile minimized.

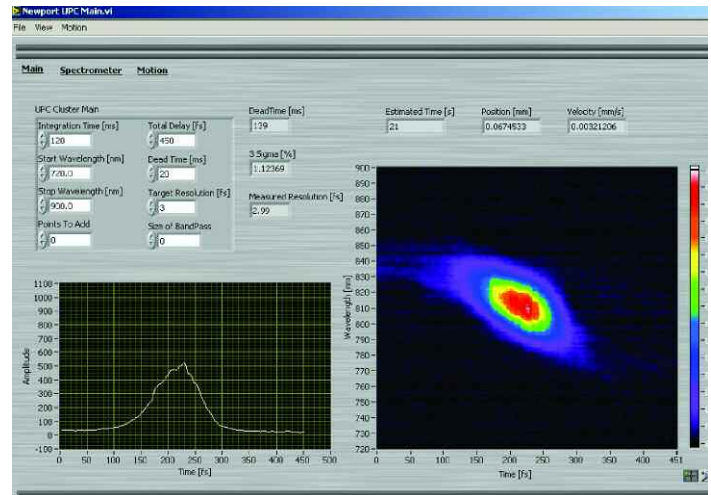


Figure 8.5 Main window. The SD FROG trace corresponds to a pulse with positive chirp.

9. Examples

After the FROG trace has been acquired, the data can be saved to a user specified folder by pressing CTRL+S. The format of the data is compatible with Femtsoft’s FROG 3.0. For the sake of ease, the file to be saved is automatically named on a time stamp basis. The name is generated in the following way: Intensity_MMDDYY_hhmmss.dat, where M = month, D = day, Y = year, h = hour, m = minute and s = second.

The data file consists of two parts: the header and the raw data separated by an empty line. The first five entries make up the header, while the remainder of the file consists of the raw data.

Alternatively, this data can be imported directly into FROG 3.0. First, select the Data Source to be the Experimental FROG Trace. Under the File containing experimental FROG trace box, enter the location and name of the file you wish to analyze and check the Use Header Information box. Select the Grid Size and NLO (SHG or SD), and then click on the OK button. The program will display of Raw Data window that gives you the option of performing math on the raw data (the Users Manual provided by Femtosoftware gives an excellent description on the functionality of this tool). After manipulation of the raw data, select the Grid Data tab and then click on the Begin button to start the phase retrieval algorithm. The program will run until interrupted by the user. When satisfied with the retrieved pulse, the user can stop the program by clicking on the Stop button, the retrieved FROG trace with the lowest error will be displayed and saved.

The FROG 3.0 software generates several files based on the retrieved pulse (again, the manual provided by Femtosoftware gives an excellent description regarding the information content of each of these files). The file that we are primarily concerned with is the speck.dat file. This file contains the spectrum of the retrieved electric field along with the phase. This file contains five columns corresponding to the following quantities: the wavelength (λ), the intensity, the phase, (ϕ in radians), and the real as well as the imaginary parts of the field. In order to determine the contributions of group delay dispersion as well as higher order dispersions to the spectral phase of the pulse, it is first necessary to convert wavelength to angular frequency, ω , with the carrier frequency subtracted out. This can be accomplished using the equation shown below:

$$\omega(\text{fs}^{-1}) = 2\pi c \left(\frac{1}{\lambda(\text{nm})} - \frac{1}{\lambda_o(\text{nm})} \right) \quad (6)$$

where c is the speed of light (300 nm/fs) and λ_o is the center wavelength. The angular frequency scale will now be in fs^{-1} . Next, it is critical to limit the spectral phase to regions which contain significant intensity. The spectral phase should be cut such that the upper and lower frequency limits correspond to the intensity of the electric field at $1/e^2$.

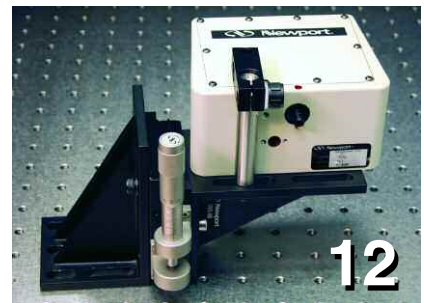
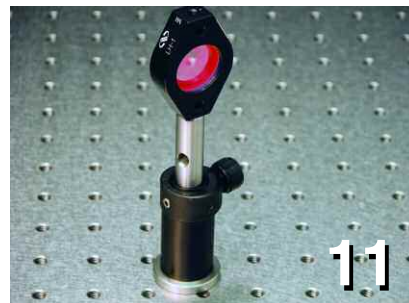
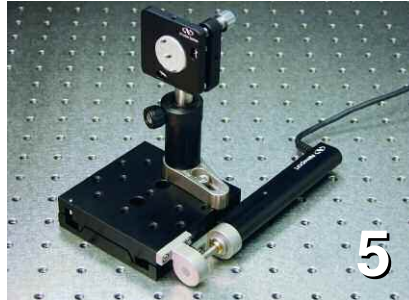
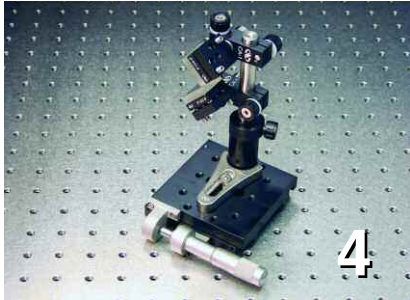
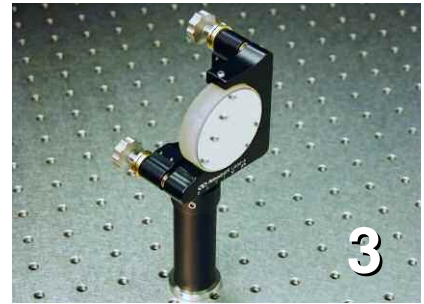
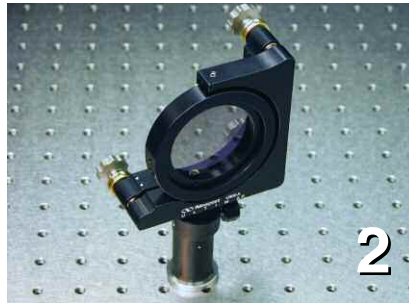
Otherwise, the phase will include artifacts from the retrieval process that will complicate this analysis. Now, the phase is displayed as a function of frequency over the spectral region containing significant intensity. Dispersion can be extracted by fitting this data to a general polynomial having the form:

$$y = a_0 + a_1x + a_2x^2 + a_3x^3 + a_4x^4 \dots, \quad (7)$$

where a_0 corresponds to phase delay, a_1 corresponds to group delay (fs), a_2 corresponds to group delay dispersion (fs^2), a_3 corresponds to third order dispersion (fs^3), and a_4 corresponds to fourth order dispersion (fs^4).

i Rick Trebino., "Frequency-Resolved Optical Grating: The Measurement of Ultrafast Laser Pulses", (Norwell, MA, Kluwer Academic Publishers, 2000)

10. Appendix – Description of Assemblies



1. Iris Diaphragm (a)
2. Beamsplitter (a) or (b)
3. Spherical Mirror
4. Delay Line 1
5. Delay Line 2
6. Folding Mirror
7. Cover Slip

8. Nonlinear Crystal
9. Iris Diaphragm (b)
10. Collimating Lens
11. Dichroic Mirror
12. Spectrometer
13. Detector

Newport Corporation

Worldwide Headquarters

1791 Deere Avenue
Irvine, CA 92606

(In U.S.): 800-222-6440

Tel: 949-863-3144

Fax: 949-253-1680

Email: sales@newport.com



Newport

Experience | Solutions



A Division of Newport Corporation

Visit Newport Online at: www.newport.com

This Application Note has been prepared based on development activities and experiments conducted in Newport's Technology and Applications Center and the results associated therewith. Actual results may vary based on laboratory environment and setup conditions, the type and condition of actual components and instruments used and user skills.

Nothing contained in this Application Note shall constitute any representation or warranty by Newport, express or implied, regarding the information contained herein or the products or software described herein. Any and all representations, warranties and obligations of Newport with respect to its products and software shall be as set forth in Newport's terms and conditions of sale in effect at the time of sale or license of such products or software. Newport shall not be liable for any costs, damages and expenses whatsoever (including, without limitation, incidental, special and consequential damages) resulting from any use of or reliance on the information contained herein, whether based on warranty, contract, tort or any other legal theory, and whether or not Newport has been advised of the possibility of such damages.

Newport does not guarantee the availability of any products or software and reserves the right to discontinue or modify its products and software at any time. Users of the products or software described herein should refer to the User's Manual and other documentation accompanying such products or software at the time of sale or license for more detailed information regarding the handling, operation and use of such products or software, including but not limited to important safety precautions.

This Application Note shall not be copied, reproduced, distributed or published, in whole or in part, without the prior written consent of Newport Corporation.

Copyright ©2007 Newport Corporation. All Rights Reserved.



Newport Corporation, Irvine, California, has been certified compliant with ISO 9001 by the British Standards Institution.

MM#00000093
DS-04074